WORK HARDENING EFFECTS ON THE MECHANICAL BEHAVIOR OF STAINLESS STEEL FASTENERS

A Thesis Presented for the

Master of Science

Degree

The University of Tennessee, Knoxville

Pierce R. Okken

December 2025

The views expressed in this article are those of the author and do not necessarily reflect the official policy or position of the Air Force, the Department of Defense or the U.S. Government.

ACKNOWLEDGEMENTS

This research was supported by the Naval Surface Warfare Center, Indian Head under Award N00174-22-1-0017. The findings, opinions, recommendations, and conclusions in this thesis are those of the author alone and do not necessarily reflect the views of others, including the sponsor.

The author thanks the following individuals from the University of Tennessee, Knoxville for their contributions to the project: Undergraduate students Arsenio Montero Alamilla, Jonathan Smith, Kaitlyn Smith, Claire Werner, and Alden Wirth; Master's students Paxton Lifsey and Alex Moore; and Technical Managers Andy Baker and Larry Roberts.

ABSTRACT

Accurate prediction of fastener strength is essential to ensure safe and efficient design. However, current design standards, such as FED-STD-H28/2B and ISO TR/16224, are largely based on data from carbon steel fasteners and do not accurately capture the behavior of stainless steel bolts, which exhibit different behavior due to work hardening during manufacturing. This thesis investigates the mechanical behavior of work-hardened stainless steel fasteners through experimental testing. Twelve lots of stainless steel bolts—spanning three material grades, multiple diameters, and manufacturing methods—were tested in tension, shear, and hardness. The results show that cold-worked stainless steel bolts consistently fail in the shank rather than the threads, confirming that threaded regions experience significant strengthening due to work hardening. Compared to FED-STD predictions, the measured tensile stress areas were on average 35% higher, while external thread shear strength was accurately captured only when using a shear-to-tensile strength ratio of 0.9 rather than the conventional 0.6. Hardness testing further revealed a 10% increase in the threaded region relative to the shank, directly evidencing nonuniform strengthening caused by cold forming. In contrast, bar-stock bolts with minimal work hardening exhibited uniform hardness, lower strength, and premature thread deformation. These findings demonstrate the critical influence of manufacturing-induced work hardening on fastener performance and provide a basis for improved predictive equations and design procedures for stainless steel bolts.

TABLE OF CONTENTS

Chapter One Introduction 1

Stainless Steel 1

Work Hardening 3

Previous Examination of Stainless Steel Bolts 4

Gaps in Knowledge 5

Scope 6

Chapter Two Strength Equations 7

Tensile Stress Area 8

Shear Area, External Threads 9

Length of Engagement 11

Chapter Three Materials and methods 14

Materials 14

Methods 16

Chapter Four Results 21

Ultimate Tensile and Yield Stress 21

Ultimate Tensile and Yield Strength 21

Tensile Stress Area 22

External Thread Shear Area 23

Shear 24

Hardness 25

Chapter Five Discussion 38
Tensile Strength 38
External Thread Shear Strength and Length of Engagement 41
Strength of Low Work Hardened Stainless Steel Bolts 41
Cross Section Hardness Comparison 47
Chapter Six Conclusions and Recommendations 50
References 52
Vita 55

LIST OF TABLES

Table 3.1. Bolt Sizes and Materials 15

Table 3.2. Nominal Strengths 16

Table 4.1. Stainless Ultimate and Yield Stress Results 26

Table 4.2. Stainless-Steel Strength Results..... 28

Table 4.3. Stainless Steel TSA Results..... 28

Table 4.4. Stainless Steel External Thread Shear Ratio..... 33

Table 4.5. Stainless Steel Shear Results 36

Table 5.1: Experimental Strength vs. Shank Area..... 39

LIST OF FIGURES

Figure 2.1. Tensile Failure 7

Figure 2.2. External Thread Shear Failure 8

Figure 3.1. Full tension testing rig 19

Figure 3.2. Shear inner bearing inserts 19

Figure 3.3. Single plane shear fixture 20

Figure 4.1. Stainless Steel (304, 304*, 18-8) Stress Comparison 27

Figure 4.2. Stainless Steel (316, 2205) Stress Comparison 27

Figure 4.3. Stainless Steel (304, 18-8) Tensile Stress Area 29

Figure 4.4. Stainless Steel (304, 18-8) Normalized Tensile Stress Area 29

Figure 4.5. Stainless Steel (304, 18-8) Tensile Stress Diameter 30

Figure 4.6. Stainless Steel (304, 18-8) Normalized Tensile Stress Diameter 30

Figure 4.7. Stainless Steel (316, 2205) Tensile Stress Area 31

Figure 4.8. Stainless Steel (316, 2205) Normalized Tensile Stress Area 31

Figure 4.9. Stainless Steel (316, 2205) Tensile Stress Diameter 32

Figure 4.10. Stainless Steel (316, 2205) Normalized Tensile Stress Diameter 33

Figure 4.11: Normalized External Thread Shear Area (304/316) 34

Figure 4.12. Normalized External Thread Shear Area (304*/18-8) 34

Figure 4.13. Normalized Length of Engagement (304/316) 35

Figure 4.14. Normalized Length of Engagement (304*/18-8) 35

Figure 4.15. Median Hardness of Shank and Threads Compared 37

Figure 4.16. 1-8 Bolts Median HRA vs Distance from Center 37

Figure 5.1. 304 Stainless 1-8 Type 0 Failure 38

Figure 5.2. L021 1-8 Type 0 Test 1 46

Figure 5.3. L021 1-8 Type 0 Test 2 46

Figure 5.4. L026 1/2-13 Type 0 Test 1 47

Figure 5.5. Stainless Steel Stress-Strain Curve Comparison 47

CHAPTER ONE

INTRODUCTION

Stainless steel bolts play an important role in enabling connections to remain safe in harsh environments by resisting strength loss through corrosion. Equations that allow designers to accurately predict the strength, safety, and efficiency of bolted fasteners are critical to engineering practice. However, the most commonly used equations for the strength of steel fasteners were developed primarily based on carbon steel and differences in behavior between carbon steel and stainless steel fasteners have been observed.

Stainless Steel

Stainless steel alloys generally fall into four main types, or "phases." These phases are determined by their crystalline structure and varying alloying element content. The following information is taken from a 2009 report in the Materials Science and Engineering Journal, by Lo et al. (2009)

Austenitic stainless steel alloys contain 17-18% Chromium and 8 to 11% nickel, but these contents can be increased to make the alloy more corrosion resistant. While carbon steels have a "body-centered cubic (BCC)" structure, austenitic stainless steels have a "face-centered cubic (FCC)" atomic structure. This unique structure allows them to be easily cold formed, making austenitic stainless steel a popular choice for structural applications. Relative to structural carbon steel, austenitic stainless steel also has better toughness over a wide range of temperatures.

The second phase is ferritic stainless steels. Ferritic stainless steel has a body-centered cubic (BCC) crystalline structure (same as carbon steel) and generally contains less chromium than austenitic stainless steel (10.5-18%) and little to no nickel. The resulting alloy is magnetic and less ductile than austenitic stainless steel. The main benefit of ferritic stainless steel is cost. The reduced nickel content significantly reduces its cost compared to austenitic stainless steel. Austenitic and ferritic stainless steel both have similar corrosion resistance.

The third phase is duplex stainless steel, which is a combination of austenitic and ferritic crystalline structures. This alloy has a microstructure with both FCC and BCC structures. Duplex stainless steel contains 20-26% chromium, 1-8% nickel, 0.05-5% molybdenum, and 0.05-3% nitrogen. The primary benefit of duplex stainless steel is a much higher strength compared to austenitic stainless steel, still retaining excellent resistance to corrosion. They have good ductility and weldability but are more difficult to form due to their high strength. Duplex stainless steel is generally the most expensive phase to produce and work.

The final phase is martensitic stainless steel. Martensitic stainless steels have BCC crystalline structure but have higher carbon content than ferritic stainless steel. Martensitic stainless steel’s unique property is that it is the only alloy that responds (strengthens) due to heat treatment. This makes it applicable for high wear uses such as knives. Compared to the other phases, martensitic stainless steels tend to be less ductile

and not as easily welded. While welding martensitic stainless steel is possible, it requires pre and post heating.

Work Hardening

Materials have different work hardening potential based primarily on the crystalline structure of their atomic lattice. Work hardening occurs because of the movement and entanglement of dislocations within the crystal lattice during plastic deformation at low temperatures (Fan et al. 1989; Koehler 1952; Wood 1940a; Zhang et al. 2006). Stainless steels, especially austenitic grades like 304 and 316, work harden much more at low temperatures than carbon steels because their FCC crystalline structure not only accumulates dislocations during deformation but also undergoes a strain-induced phase transformation. This dual mechanism greatly increases their strength while maintaining good ductility. In contrast, carbon steels harden mainly through dislocation buildup alone, and their body-centered cubic structure allows some recovery that limits the overall hardening effect. As a result, carbon steels show moderate increases in strength and lose ductility, while austenitic stainless steels can nearly double their strength through cold working and remain highly formable (Atkinson 1984; Dolinšek 2003; Fan et al. 1989; Koehler 1952; Wood 1940b).

Cold working of bolts occurs in several different steps in manufacturing process, including straightening from coil and forming the threads. Straightening from coil cold works the entire length of the bolt while forming the threads is cold works just the threaded length. The degree of cold working can differ between manufactures and

producers. Machining threads does not cold work the material as forming the threads as material is removed and not deformed.

To distinguish between materials that have the potential to see significantly increased strengths and those that have undergone the cold-working necessary to realize those increased strengths, this thesis uses the terms “work hardening potential (WHP)” and “realized work hardening (RWH)”. The term work hardening potential refers to a materials ability to work harden. Since work hardening can be induced to varying degrees through the manufacturing process, the actual work hardening a material receives during manufacture referred to as its realized work hardening.

Previous Examination of Stainless Steel Bolts

Stainless steel bolts, when tested in tension, have been known to fail in the shank rather than the threaded portion where the area is lower. Song, et al. (2020) and Stranghöner and Abraham (2021) observed this behavior in full-size tensile tests of high-strength austenitic stainless steel bolts, which consistently failed through the unthreaded shank rather than through the threads. The authors hypothesized that this unexpected failure mode was caused by a non-uniform distribution of material properties along the bolt, with the threads being substantially strengthened during manufacturing.

Stranghöner and Abraham (2021) further documented this phenomenon in their investigation of the behavior of austenitic stainless steel bolts under tension. They reported that stainless steel bolts typically fail in the shank region, while carbon steel and

duplex stainless steel bolts fail in the threaded region corresponding to the tensile stress area.

The metallurgical mechanisms behind this behavior have been recognized for many years. Llewellyn (1997) noted that the tendency of austenitic stainless steels to undergo strain-induced martensitic transformation during cold working has been well documented for over half a century. The martensitic transformation occurs mainly near where the material experiences the greatest strain during working, resulting in locally increased hardness and tensile strength (Cook 1987), which in bolts would be near the edges of the threads. In contrast, the shank region remains largely unaffected by this transformation and retains lower strength, making it the location of failure under tensile loading. He also emphasized that the degree of work hardening depends strongly on alloy composition. More highly alloyed austenitic stainless steels are more resistant to martensitic transformation and therefore experience less work hardening during manufacturing. As a result, these alloys tend to maintain more uniform material properties throughout the bolt cross-section and benefit less from the strengthening effects associated with cold working.

Gaps in Knowledge

While previous research has documented shank failures in stainless steel bolts loaded in tension and has proposed a cause, gaps in knowledge remain. The external thread shear strength of stainless steel bolts is undocumented and the impact of cold working on the required length of engagement is unclear. Further, while work hardening

is a likely cause for the difference in behavior between stainless steel and carbon steel bolts, there is little direct evidence that this is the case.

Scope

This thesis seeks to fill these gaps in knowledge through experimental testing. Experimental data was measured for 12 different lots of stainless steel bolts as part of a larger study on the strength of metallic fasteners. Over the 12 different lots, there are three different material grades (304/18-8, 316, and 2205 duplex), two manufacture types (from coil and from bar stock), and four different sizes. A variety of tests were performed including tension testing, shear testing, and hardness testing. Included in the tension testing were experiments to assess the external thread shear strength, providing information on the length of engagement required to achieve tensile failure.

To corroborate the theory that work hardening is the cause of the differences in behavior between stainless steel and carbon steel bolts, tests were performed on bolts with different levels of cold working and hardness testing was performed in the shank and in the threads. The results of these demonstrate the difference in mechanical behavior between work-hardened and un-work hardened stainless steel fasteners.

Furthermore, the tests provide additional high-quality data to enable statistical evaluation of the strength of stainless steel fasteners. In all, this work advances the understanding of work hardening effects in stainless steel bolts and enables evaluation towards more efficient design.

CHAPTER TWO

STRENGTH EQUATIONS

Three distinct failure modes for bolts in pure tension exist: tensile failure of the bolt (typically through the threaded section) perpendicular to the load (**Figure 2.1**), shear failure in the bolt threads parallel to the load (**Figure 2.2**), and shear failure in the nut threads parallel to the load**.** The strength of the threaded parts in each of these failure modes depends on the geometry of the threads and the material properties of the bolt and the nut. For pure shear, only one mode exists, the bolt shears along the line between the connected parts, this failure can either happen through the threaded portion or through the shank.

Equations for the tensile strength of bolts are presented in several standards including FED-STD H28/2B (GSA 1991) and ISO TR/16224 (ISO 2012). Hereafter, these standards will be referred to as FED-STD and ISO, respectively.

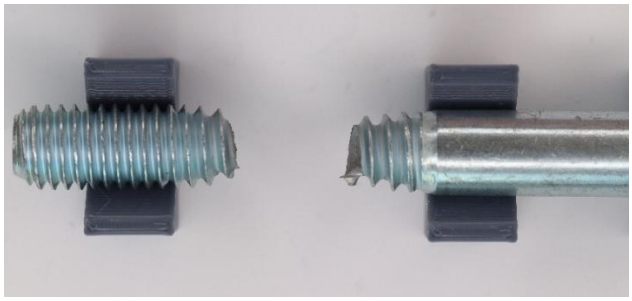


Figure 2.1. Tensile Failure

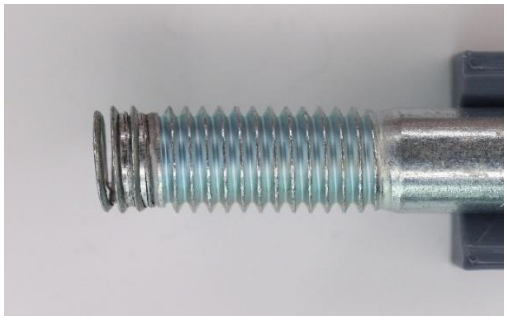


Figure 2.2. External Thread Shear Failure

Tensile Stress Area

Tensile strength for the limit state of tensile failure in these standards is equal to the circular tensile stress area times the tensile strength of the bolt material. FED-STD notes that “tests have shown that externally threaded parts fail in tension at loads corresponding to those of unthreaded parts with diameters midway between their pitch diameter and their minor diameters”. The standard includes two formulas for tensile stress area that “have been applied successfully to steel and other materials with ultimate strengths up to 180,000 psi”. **Equation 2.1** and **Equation 2.2** are listed in FED-STD Table II.B.1 as Formulas (1a) and (1b), respectively.

$$A_s = \pi \left(\frac{d_{2,bsc}}{2} - \frac{3H}{16} \right)^2$$

Equation 2.1

$$A_s = \frac{\pi}{4}\left(d_{bsc} - \frac{9\sqrt{3}}{16n} \right)^2$$

Equation 2.2

Shear Area, External Threads

Equations for the thread shear area of bolts are also presented in these standards. Thread shear area in these standards is an effective cylinder through the threads. Equations for thread shear strength are provided in ISO, equal to the thread shear area times the shear strength of the failing material, i.e., the shear strength of the bolt for external failure and the shear strength of the nut for internal failure.

FED-STD notes that "the geometric shear area of an external thread at minimum material is equal to the area of that thread which is intersected by a cylinder with a diameter equal to the maximum minor diameter of the mating internal thread" over the length of engagement. The standard includes two formulas for this area.

$$AS_{s,min} = \pi n D_{1,max} \left[\frac{1}{2n} + \frac{1}{\sqrt{3}} \left(d_{2,min} - D_{1,max} \right) \right] LE$$

Equation 2.3

$$AS_{s,min} = \pi D_{1,max} \left[\frac{3}{4} - \frac{n}{\sqrt{3}} \left(TD_1 + Td_2 + es \right) \right] LE$$

Equation 2.4

A simplified formula, **Equation 2.5**, based on uncited empirical data is also included.

$$AS_{s,min} = \pi d_{2,bsc} \frac{5}{8} LE$$

Equation 2.5

Equation 2.3, Equation 2.4, and **Equation 2.5** are listed in FED-STD Table II.B.1 as Formulas (4a), (4b), and (5), respectively.

FED-STD includes additional equations for the shear area of external threads at basic size, $AS_{s,max}$. Two formulas are given in FED-STD Table II.B.1 and labeled (6a) and (6b). Formula (6a) references a chart of nominal minimum length of engagement. Formula (6b) is shown here as **Equation 2.6**.

$$AS_{s,max} = \pi D_{1,bsc} \frac{3}{4} LE$$

Equation 2.6

Equation 2.6 is used when calculating the required length of engagement based on shear of internal thread.

The equation for shear area of external threads in ISO is given as **Equation 2.7**.

$$AS_s = 0.6 m_{eff} \pi n D_1 \left[\frac{1}{2n} + \frac{1}{\sqrt{3}} (d_2 - D_1) \right] + 0.4 m_{eff} \pi n D_m \left[\frac{1}{2n} + \frac{1}{\sqrt{3}} (d_2 - D_m) \right]$$

Equation 2.7

where $D_m = 1.026 D_1$ and m_{eff} is the effective nut height. It should be noted that in this study, the chamfers were sawn off both the bolt and nut, resulting in a flat surface. Because of this, in this equation, $m_{eff} = m$.

Equation 2.7 is similar in form to **Equation 2.3** with the exception of an adjustment to the minor diameter of the nut over a portion of the nut height to account for the bell-mouthing. Bell-mouthing is the gradual taper of the internal threads that can occur during machining. **Equation 2.7** also explicitly accounts for chamfers.

Length of Engagement

FED-STD notes that if failure occurs, "it is generally more economical that the externally threaded part will break rather than that either the external or internal thread will strip." To achieve this condition, the standard provides several formulas for the length of engagement such that the tensile strength of the bolt is less by a margin than either the internal or external thread shear strength. For clarity, the required length of engagement such that tensile rupture controls the strength of the bolt is denoted as LE_r in this document.

The use of the several equations for LE_r in FED-STD depends on the relative strengths of the internally threaded part and the externally threaded part defined as R_1/R_2. R_1 and R_2 are defined in **Equation 2.8** and **Equation 2.9**, respectively.

$$R_1 = \frac{AS_{s,max}}{AS_{n,min}}$$

Equation 2.8

where $AS_{s,max}$ is determined using **Equation 2.6** or FED-STD Table II.B.1 Formula (6a) and $AS_{n,min}$ is determined using **Equation 2.10** or **Equation 2.11** (in this work only **Equation 2.11** is used).

$$R_2 = \frac{UTS_n}{UTS_s}$$

Equation 2.9

$$AS_{n,min} = \pi n d_{min}\left[\frac{1}{2n} + \frac{1}{\sqrt{3}}\left(d_{min} - D_{2,max}\right)\right]LE$$

Equation 2.10

$$AS_{n,min} = \pi d_{min}\left[\frac{7}{8} - \frac{n}{\sqrt{3}}\left(Td + TD_2 + es\right)\right]LE$$

Equation 2.11

Equation 2.8 and **Equation 2.10** are listed in FED-STD Table II.B.1 as Formulas (8) and (9), respectively.

If $R_1/R_2 \approx 1$, then combined external and internal thread shear failure is assumed to control and **Equation 2.12** is used to determine LE_r. **Equation 2.12** is listed in FED-STD Table II.B.2 as Formula (13). No definition for how close R_1/R_2 needs to be to 1 for **Equation 2.12** is provided in the FED-STD.

$$LE_r = \frac{4A_s}{\pi d_{2,bsc}}$$

Equation 2.12

Where, A_s is calculated from either **Equation 2.1** or **Equation 2.2.**

If $R_1/R_2 < 1$, then exterior thread shear failure is assumed to control and **Equation 2.13** is used to determine LE_r. **Equation 2.13** is listed in FED-STD Table II.B.2 as Formula (14).

$$LE_r = \frac{2A_s}{AS_{s,min} / LE}$$

Equation 2.13

where, A_s is calculated from **Equation 2.1** or **Equation 2.2**, and $AS_{s,min}/LE$ is calculated from **Equation 2.3** or **Equation 2.4**.

If $R_1/R_2 > 1$, then internal thread shear failure is assumed to control and **Equation 2.14** is used to determine LE_r. **Equation 2.14** is derived from FED-STD Table II.B.2 Formulas (15) and (16).

$$LE_r = \frac{2A_s}{AS_{s,max} / LE} \frac{R_1}{R_2}$$

Equation 2.14

where, A_s is calculated from either **Equation 2.1** or **Equation 2.2** and $AS_{s,max}/LE$ is calculated from **Equation 2.6**.

CHAPTER THREE

MATERIALS AND METHODS

Several types of tests were performed to quantify the behavior and strength of stainless steel fasteners, including: full tension tests: tests with internally threaded part of sufficient length of engagement and unmodified bolt to evaluate bolt tensile strength; reduced diameter tension tests: tests with internally threaded part of sufficient length of engagement and reduced diameter bolt to evaluate bolt material properties; external thread shear tests: tests with flattened strong nut and bolt with removed chamfer to evaluate external thread shear strength; shear tests: tests with consumable bearing inserts and a 90^{o} shear plane to evaluate bolt shear strength in the threads and shank; and hardness tests: hardness of the bolt cross section was tested on multiple spokes across the face using HRA procedures.

Materials

A variety of fastener materials and sizes were tested as summarized in **Table 3.1**. For consistency and to minimize material variability, all specimens within a given lot originated from the same production batch. Testing was conducted on three different grades of stainless steel: Grade 304/18-8, Grade 316, and 2205 Duplex. Twelve lots were tested across these three grades in four sizes, all with coarse (UNC) threads. The bolts conformed to mechanical properties specified by ASTM F593-2017, ASME/ASTM A182, ASME/ASTM A276, and ASME/ASTM A479. Grades 304 and 18-8 are grouped together, as they refer to the same material under different naming conventions.

Table 3.1. Bolt Sizes and Materials

Lot Number	UN Size	Pitch (mm)	d_{bsc} (mm)	Material	Length (mm)	Manufacturer
L015	1/4-20	1.27	6.35	304	101.6	A
L016	1-8	3.175	25.4	304	177.8	A
L017	1/4-20	1.27	6.35	316	101.6	A
L018	1/2-13	1.95	12.7	316	101.6	A
L019	3/4-10	2.54	19.05	316	152.4	A
L020	1-8	3.175	25.4	316	177.8	A
L021	1-8	3.175	25.4	ASTM A193 B8M	177.8	B
L026	1/2-13	1.95	12.7	ASTM A193 B8M	101.6	B
L032	1/2-13	1.95	12.7	18-8	101.6	A
L033	3/4-10	2.54	19.05	18-8	152.4	A
L034	1-8	3.175	25.4	18-8	177.8	A
L035	1/2-13	1.95	12.7	2205 Duplex	101.6	C

For tension tests, unless otherwise noted, fabricated internally threaded parts were custom machined out of 4140 pre-hardened steel to fit manufactured fixtures for an Instron Universal Testing Machine and with internal thread dimensions which matched the tested bolts. These threaded parts were fabricated so that the length of engagement and internal thread shear strength did not control and the desired method of tensile failure in the bolt was achieved.

Nominal strength properties for each bolt material used are listed in **Table 3.2**. This data sourced from the website MatWeb (MatWeb 2025). Note that these nominal strengths are assumptions made in design and are only used as a point of comparison. It is assumed that each design entity uses its own nominal strength assumptions gathered from previous experience, standards, or testing. Material testing following the procedures described in this chapter was conducted on all materials to quantify material strengths.

Table 3.2. Nominal Strengths

Material	Nominal Yield (PSI)	Nominal Ultimate (PSI)	UNS
304 Stainless	31200	73200	S30400
316 Stainless	30000	75000	S31600
2205	67000	90000	S32205

Methods

The tension and shear tests described in this thesis were done in general accordance with ASTM F606 (ASTM 2021) which describes standard test methods for bolts. All tension and shear tests were deformation controlled with a rate of crosshead movement equal to 0.05 in./min. for 1/4 in. bolts and 0.1 in./min. for the larger sizes.

Full specimen tension tests were the most basic test type and were completed in accordance with Section 3.4 of ASTM F606 (ASTM 2021). These were designed to achieve tensile failure. An axial extensometer was attached to the bolt during testing and kept on through the ultimate load, but was removed before failure. Five bolts were tested from each lot. The fixture for full specimen and reduced diameter tension tests can be seen in **Figure 3.1**.

Reduced diameter tension tests were essentially coupon tests and were completed in accordance with Section 3.6 of ASTM F606 (ASTM 2021). The shank of the bolts were machined to conform with ASTM E8 (ASTM 2022). A miniature axial extensometer was attached to the reduced shank during each test, and was left on through the ultimate load but removed before failure. Five bolts were tested from each lot.

External thread shear tests used reduced lengths of engagement in order to ensure thread shear failure. This type of test is not described in ASTM F606 (ASTM 2021). For external thread shear failure, grade 2H heavy hex nuts (hereafter called strong nuts) were used as the internally threaded part. These nuts have a minimum tensile strength of 180,000 psi, which was confirmed to be reasonable based on hardness testing. The chamfered ends of the bolt and the strong nut were removed to prevent partial threads in these regions from affecting the strength of the bolt. Target lengths of engagement were calculated using the material strength of the bolt lot as determined in the reduced diameter tests. These targeted lengths of engagement were achieved by placing a gage ball inside the strong nut against the flat end of the bolt. The strong nut was then tightened until a straight edge against the face of the strung nut contacted the gage ball. An extensometer could not be used effectively during these tests as thread shear failure is too brittle to allow a reliable window during which the test could be paused and the extensometer removed. Ten bolts were tested from each lot; five at each target length of engagement of 37.5% and 75% of the calculated required length of engagement.

Shear tests were completed in accordance with Section 3.8 of ASTM F606 (ASTM 2021) and used a shear rig comprised of two halves, each containing an inner and outer bearing all made of 4140 pre-hardened steel to test the bolts in single-plane shear, as seen in **Figure 3.2** and **Figure 3.3**. The inner sacrificial bearing surfaces were replaced following each test to ensure a single, continuous shear plane through the bolt and reduce material fatigue on the larger portions of the testing rig. Attached to the side of the shear

rig were two linear variable differential transformers (LVDT) to provide displacement data throughout the test. For each test, the bolt would be inserted into the appropriately sized insert and secured with spacers and a nut to ensure the correct portion (threads or shank) remained in the shear plane for the duration of the test. Testing would conclude when the bolt reached shear failure and was "cut" into two halves. For each lot, 5 shear tests were performed in the threads, and 5 shear tests were performed in the shank.

Hardness testing conformed to ASTM E18 (ASTM 2025) and ASTM F606 Section 3.1 (ASTM 2021). For each selected lot for hardness testing, 10 bolt specimens were cut into 2 sections. One section was cut from the center of the threads and one from the center of the shank. These test rounds were faced to ensure flatness and then tested with a Rockwell Hardness A (HRA) procedure. Testing began in the center of the cross section and continued towards the edge in 4 different "spokes", each 90 degrees to the next. Tests interval was set to 0.05 inches and continued until at least one of the spokes reached the edge of the section. In total, for each lot, 20 sections were tested (10 threaded, 10 unthreaded), with the total amount of individual hardness tests varying by the diameter of the bolt.



Figure 3.1. Full tension testing rig

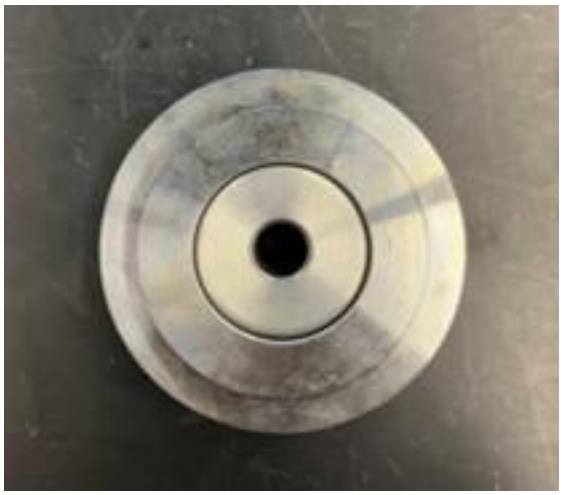


Figure 3.2. Shear inner bearing inserts

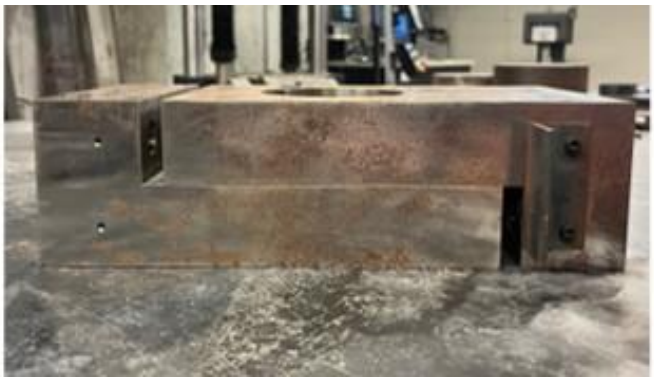


Figure 3.3. Single plane shear fixture

CHAPTER FOUR

RESULTS

Ultimate Tensile and Yield Stress

Ultimate tensile and yield stress for each lot of bolts was derived from the results of the reduced diameter tension tests. The results are presented in **Table 4.1**, **Figure 4.1**, and **Figure 4.2**.. The table lists the nominal ultimate stress from **Table 3.2,** the ultimate stress listed on the material certification for the lot, and the measured ultimate stress, and the measured yield stress. Ratios between the measured ultimate stress and both the nominal and material certification values are also tabulated. The figures display the measured yield and ultimate stress by lot including error bars that represent the 90% confidence interval of the mean.

Ultimate Tensile and Yield Strength

Ultimate tensile and yield strength for each lot of bolts was derived from the results of the full specimen tension tests. The results are presented in **Table 4.2**. The table lists the measured ultimate strength, measured yield strength, the ratio of yield to ultimate, as well as the location of the failure. Note that results for lots L021 and L026 are not shown, as these specimens could not be failed in tension. This phenomenon is discussed further in Chapter 5.

Tensile Stress Area

The experimental tensile stress area was calculated as the average load from the full specimen tension tests divided by the average material strength from reduced diameter tension tests.

$$TTSA = \frac{Peak\ Load}{UTS_s}$$

Equation 4.1

The results are presented in **Table 4.3**, which lists the test tensile stress area (*TTSA*) and the FED-STD tensile stress area (FSTSA).

This section also contains several plots comparing the experimental results to the predicted tensile stress area for each lot of bolts tested. The error bars in these figures represent the propagated uncertainty using the 90% confidence intervals from reduced diameter and full specimen tension tests. The first plot presents the results as calculated. Each progressive plot normalizes the data in various ways. First the results are divided by the nominal area. Then, the results are recalculated as the tensile stress diameter by solving the equation of circular area for diameter. The y-axis for this plot is presented in fractions of *H*, the height of the sharp v-thread. This was to make comparison to the tensile stress area equations easier, as they adjust the tensile stress area circle with some fraction of *H*. In total, 4 plots are generated for each grouping of bolts: Tensile Stress Area, Normalized Tensile Stress Area, Tensile Stress Diameter, and Normalized Tensile Stress Diameter. **Figure 4.3** through **Figure 4.6** contain the normalized plots for the 304 and 18-8 bolt sizes while **Figure 4.7** through **Figure 4.10** contain the plots for 316 and

2205. Note that once again Lots L021 and L026, the 304* B8M lots, are once again missing as they did not fail tension.

External Thread Shear Area

The effects of work hardening on external thread shear area (ETSA) and length of engagement can be quantified through comparison to the FED and ISO standards. It should also be noted that in these calculations, instead of using the standard shear strength of $0.6F_u$ (60% tensile strength), the shear strength was taken to be $0.9F_u$ based on the shear data presented in **Table 4.5**.

A series of graphs were generated for the results of the external thread shear tests. First, on a lot-by-lot basis, the strengths for the tests at each target length of engagement were grouped together and the 90% confidence interval was calculated. A linear regression was then performed with the mean of these confidence intervals and the origin on axes of strength vs length of engagement. The FED-STD equation line was evaluated at the minimum material condition and without including the correction for chamfer or bell mouthing (as the chamfer on both the bolt and nut were removed). Both graphs included a linear regression with the confidence intervals and the mean ultimate tensile strength from full specimen tension tests. All values were normalized by nominal diameter, d_{bsc}.

From these initial graphs, a ratio was calculated between the slope of the 90% confidence interval linear regression of the tests and the slope of the FED-STD equation. This ratio was determined for each lot and presents whether the lot, on average, achieved

higher or lower strengths than the FED-STD equation results at each length of engagement.

Two more graphs were made. The slope of the linear regression is divided by the material strength of the lot, giving the tensile stress area per unit length of engagement. A second instance of the ISO equation is included, this time multiplied by appropriate *C*-factors, C_1 and C_2. All of these values are normalized by nominal diameter, d_{bsc}. The experimental ultimate tensile load was divided by the slope of the linear regression to achieve an estimation of the experimental length of engagement. The predicted length of engagement per FED-STD and the length of engagement predicted by ISO found through reverse engineering were also included. All values were again normalized by nominal diameter, $d_{bsc.}$

An important note, the value of C_2 depends on R_s as defined in ISO Section 4.2.3.1, but C_2 is defined only for $R_s < 2.2$. For lack of a better approach, if $R_s > 2.2$, then C_2 was taken as 1.1415 (i.e., the value of C_2 when $R_s = 2.2$).

The FED-STD ratio for each stainless steel lot is presented in **Table 4.4**, and the graphs are presented in **Figure 4.11, Figure 4.12, Figure 4.13,** and **Figure 4.14**. The table is broken into two sections, with Lots L021 and L026 separated, as these two lots behaved in a unique manner, uncharacteristic of the other stainless lots.

Shear

To determine the shear ratio, the ultimate load for each specimen was used to find the average ultimate load for each specimen in the threads and in the shank. The ultimate

in the threads was then divided by the ultimate in the shank to determine the shear ratio of the bolt. Using this shear ratio, the shear area in the threads was then calculated by taking the shear ratio times the area in the shank. The area in the shank was calculated from the body diameter measurements taken before testing. No yield strength was calculated in the shear tests. The ultimate stress was calculated by the shank peak load divided by the measured shank area.

The results for each material type are presented in **Table 4.5**. The table lists the average shear ultimate load for the shank and threads, the ultimate stress of that load in the shank, the ratio of the ultimate load in the threads to the shank, and the ratio of the shear ultimate stress to the tensile ultimate stress found in the reduced diameter tension tests.

Hardness

To analyze the HRA hardness testing results, a bar chart compares the median HRA hardness value of the threaded portion to the unthreaded portion of a specimen (**Figure 4.15)**. Median was chosen to eliminate outliers in the data. Error bars show the interquartile range of the data, and a percentile label gives the percent difference between the threads and the shank median. A plot of median HRA hardness vs. distance from center for two 1-8 bolts (304* and 304) is also shown in **Figure 4.16**.

Before presenting the median hardness data, it should be noted that the ¼-20 bolts presented a high level of difficulty to achieve repeatable hardness data. The smaller cross

section provides little margin for error in mounting and resulting hardness data was very noisy.

Table 4.1. Stainless Ultimate and Yield Stress Results

	All values in Pounds Per Square Inch (PSI)				
Lot	**Nominal Ultimate**	**Cert Ultimate**	**Test Ultimate**	**Test Yield**	**Nom. Ult. Ratio**
L015: 304 1/4-20	73200	141000	100288	64856	1.37
L016: 304 1-8	73200	113000	93478	52906	1.28
L017: 316 1/4-20	75000	142000	99023	63983	1.32
L018: 316 1/2-13	75000	135000	103735	67969	1.38
L019: 316 3/4-10	75000	112000	87007	53908	1.16
L020: 316 1-8	75000	111000	89845	53988	1.20
L021: B8M 1-8	73200	92000	83505	38528	1.14
L026: B8M 1/2-13	73200	82500	81001	36863	1.11
L032: 18-8 1/2-13	73200	128000	100476	60964	1.37
L033: 18-8 3/4-10	73200	114000	94347	55540	1.29
L034: 18-8 1-8	73200	112000	92173	51389	1.26
L035: 2205 1/2-13	90000	111534	118391	102505	1.32
				Mean	**1.27**
				Std. Dev.	**0.095**

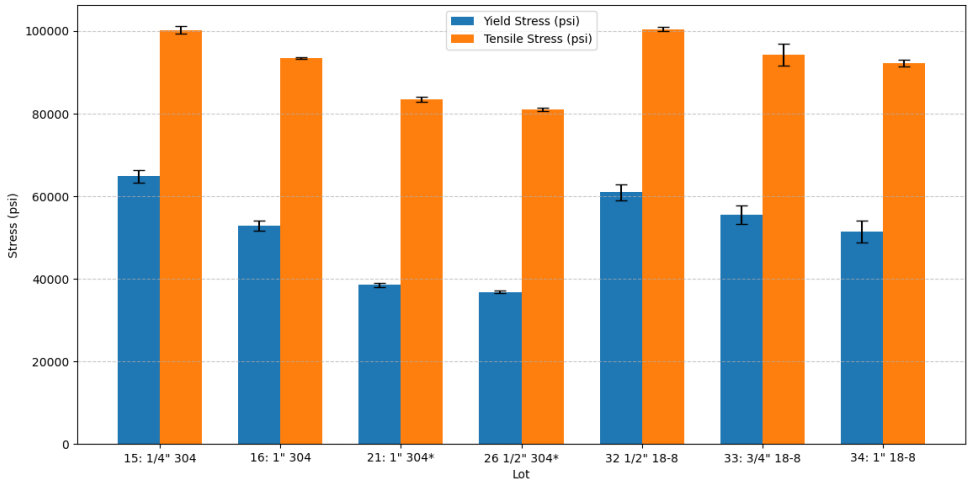


Figure 4.1. Stainless Steel (304, 304*, 18-8) Stress Comparison

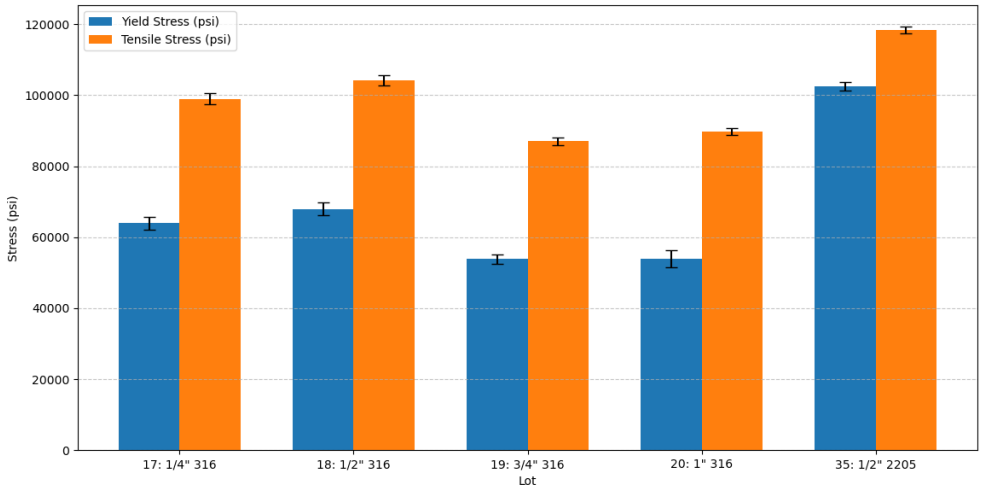


Figure 4.2. Stainless Steel (316, 2205) Stress Comparison

Table 4.2. Stainless-Steel Strength Results

	In Pounds			
Lot	**Peak Load**	**Yield Load**	**Y_L/P_L Ratio**	**Failure Mode**
L015: 304 1/4-20	4689	2447	0.522	Shank
L016: 304 1-8	71578	38287	0.535	Shank
L017: 316 1/4-20	4656	2758	0.592	Shank
L018: 316 1/2-13	19836	11700	0.590	Shank
L019: 316 3/4-10	39285	22791	0.580	Shank
L020: 316 1-8	69316	40470	0.584	Shank
L032: 18-8 1/2-13	19026	10481	0.551	Shank
L033: 18-8 3/4-10	40248	21383	0.531	Shank
L034: 18-8 1-8	71367	40893	0.573	Shank
L035: 2205 Duplex 1/2-13	18213	15435	0.847	Threads

Table 4.3. Stainless Steel TSA Results

	In in^2		
Lot	**TTSA**	**FSTSA**	**TTSA/FSTSA**
L015: 304 1/4-20	0.047	0.030	1.551
L016: 304 1-8	0.766	0.600	1.276
L017: 316 1/4-20	0.047	0.031	1.521
L018: 316 1/2-13	0.191	0.139	1.377
L019: 316 3/4-10	0.452	0.332	1.363
L020: 316 1-8	0.772	0.602	1.283
L032: 18-8 1/2-13	0.189	0.137	1.377
L033: 18-8 3/4-10	0.427	0.327	1.306
L034: 18-8 1-8	0.774	0.584	1.324
L035: 2205 Duplex 1/2-13	0.154	0.138	1.118
		Mean	**1.350**
		Std. Dev.	**0.1237**

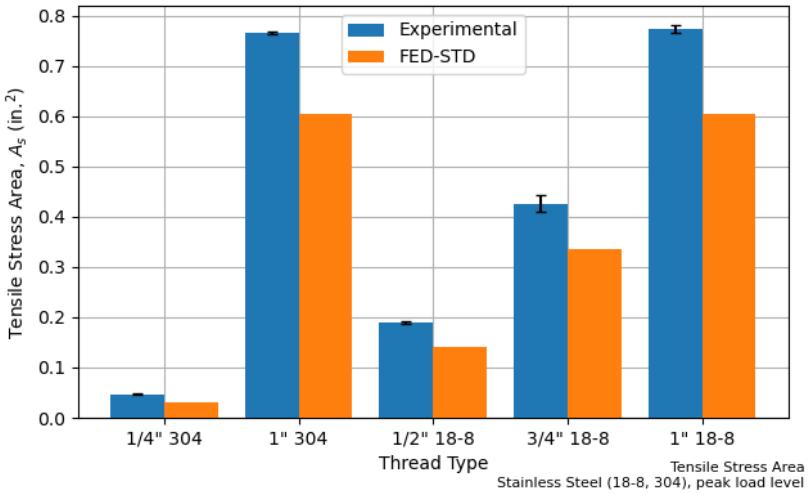


Figure 4.3. Stainless Steel (304, 18-8) Tensile Stress Area

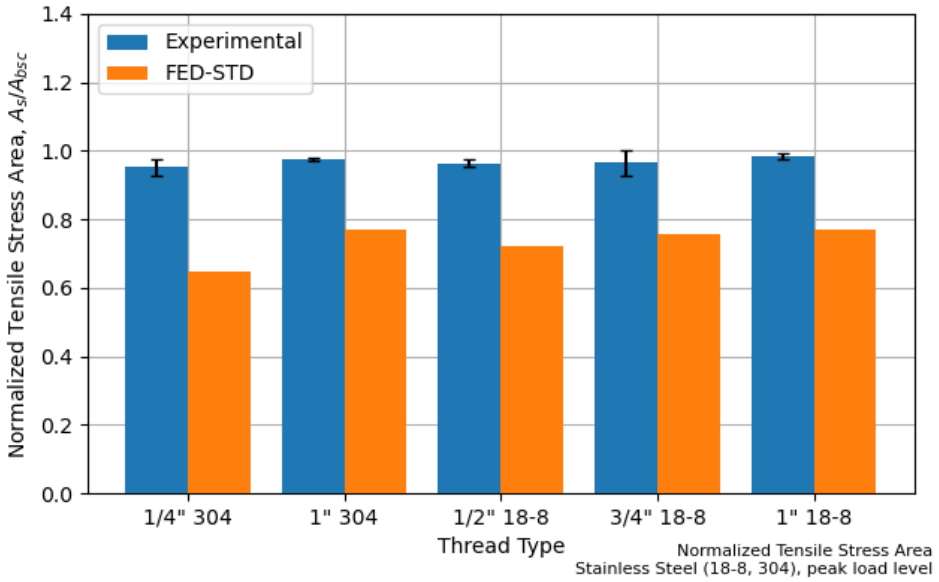


Figure 4.4. Stainless Steel (304, 18-8) Normalized Tensile Stress Area

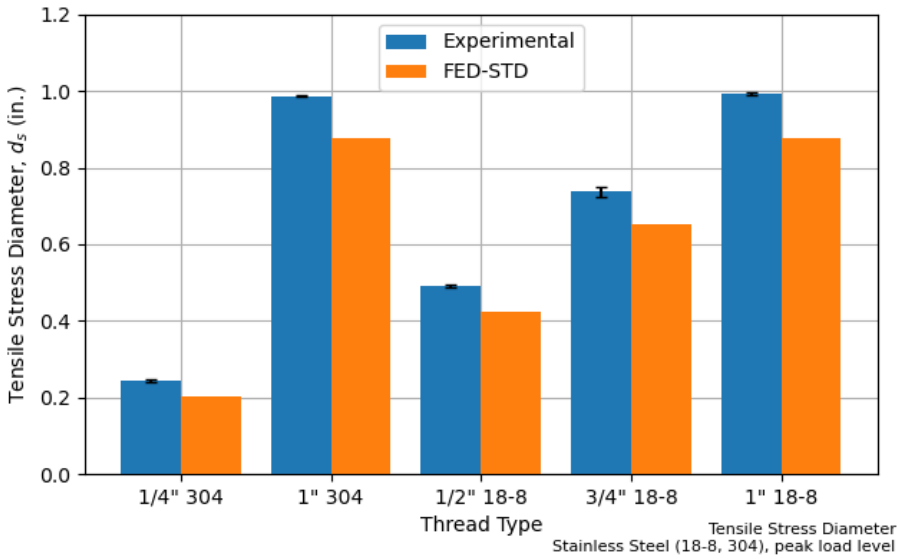


Figure 4.5. Stainless Steel (304, 18-8) Tensile Stress Diameter

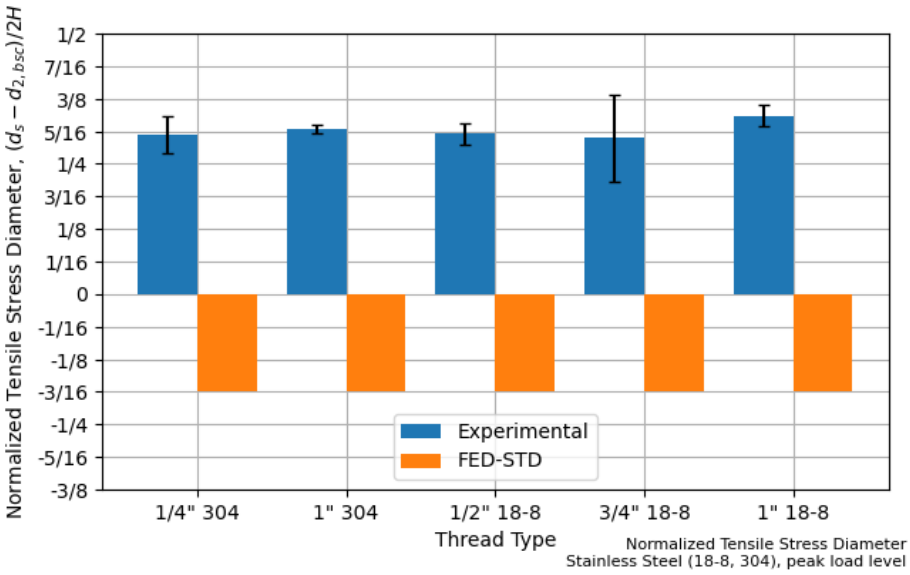


Figure 4.6. Stainless Steel (304, 18-8) Normalized Tensile Stress Diameter

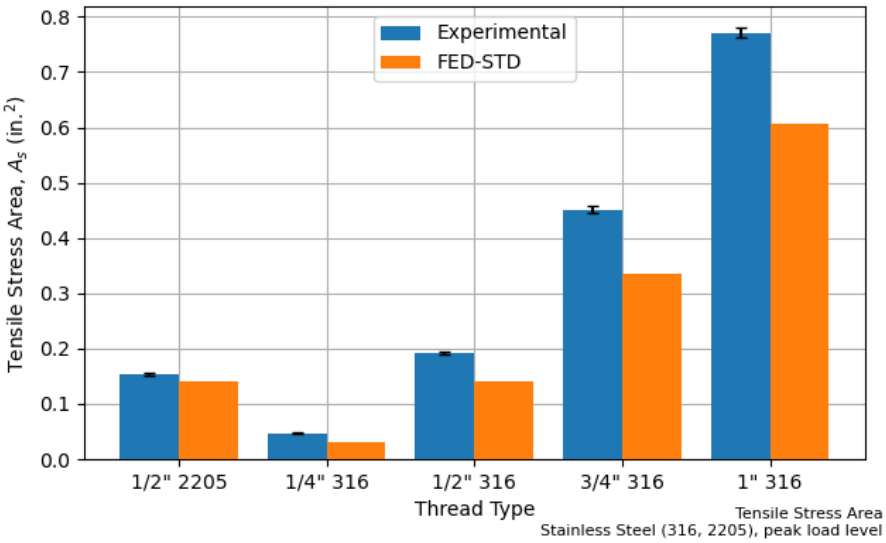


Figure 4.7. Stainless Steel (316, 2205) Tensile Stress Area

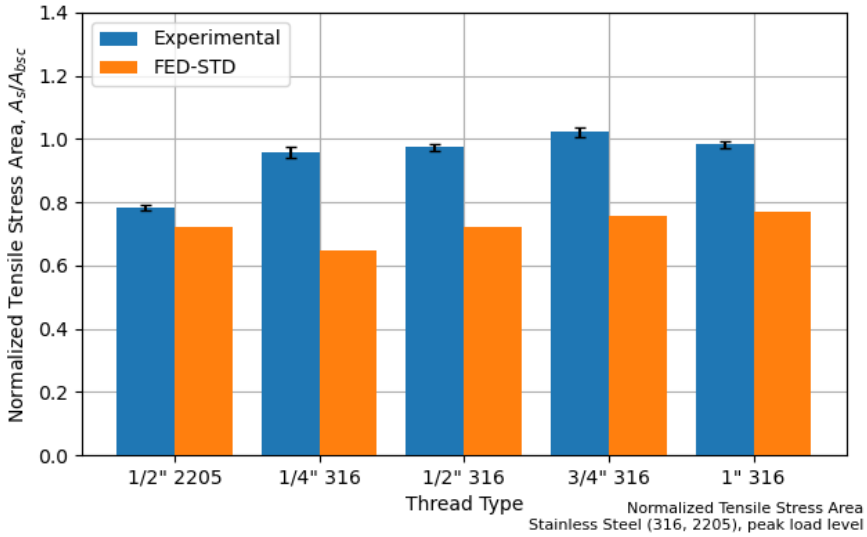


Figure 4.8. Stainless Steel (316, 2205) Normalized Tensile Stress Area

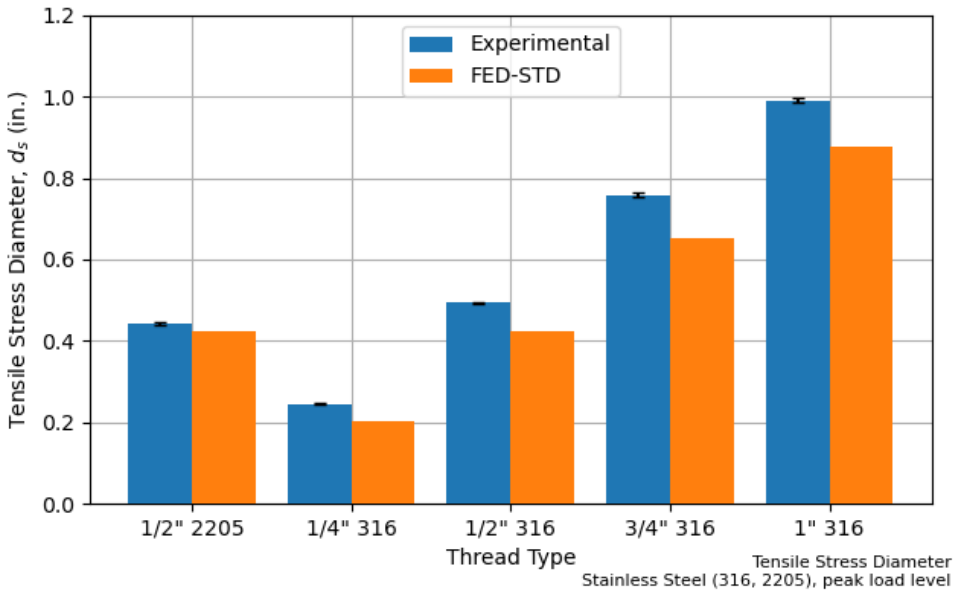


Figure 4.9. Stainless Steel (316, 2205) Tensile Stress Diameter

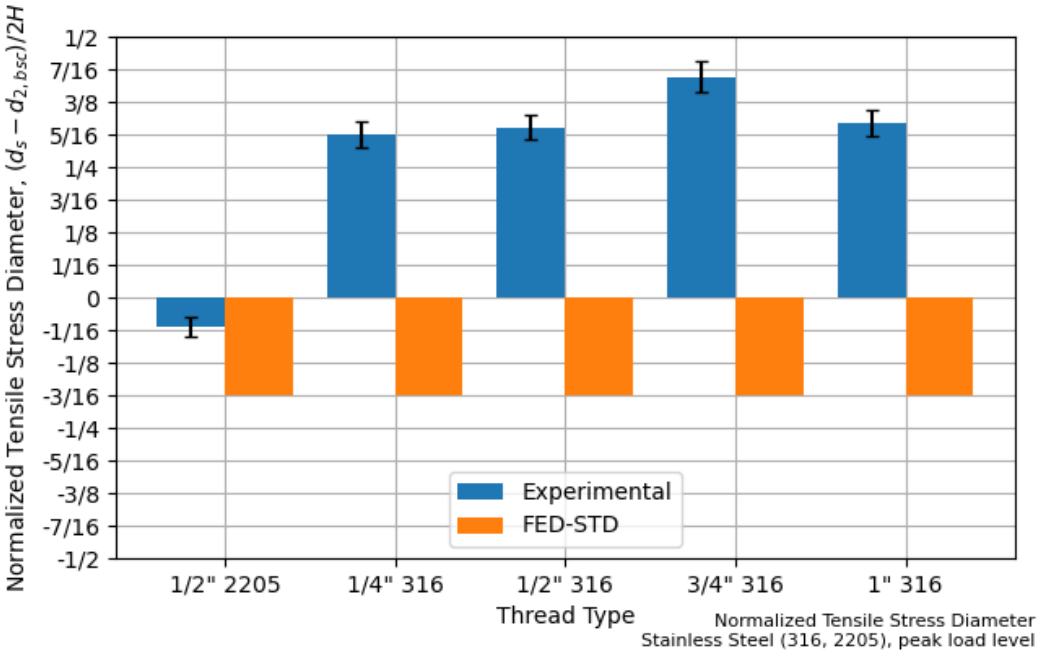


Figure 4.10. Stainless Steel (316, 2205) Normalized Tensile Stress Diameter

Table 4.4. Stainless Steel External Thread Shear Ratio

Lot	Ext. Thread Shear Ratio
L015: 304 1/4-20	0.889
L016: 304 1-8	1.070
L017: 316 1/4-20	0.893
L018: 316 1/2-13	0.974
L019: 316 3/4-10	1.150
L020: 316 1-8	1.095
L032: 18-8 1/2-13	1.029
L033: 18-8 3/4-10	0.800
L034: 18-8 1-8	1.114
L035: 2205 Duplex 1/2-13	0.812
Mean	**0.983**
STD	**0.121**
L021: ASTM A193 B8M 1-8	0.588
L026: ASTM A193 B8M 1/2-13	0.550
Mean	**0.569**
STD	**0.019**

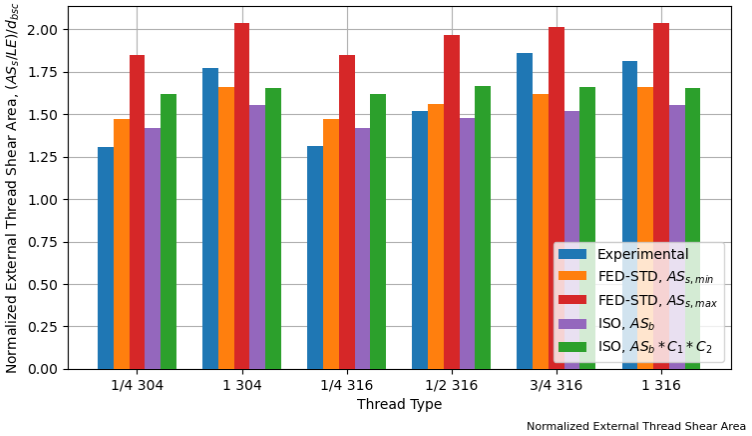


Figure 4.11: Normalized External Thread Shear Area (304/316)

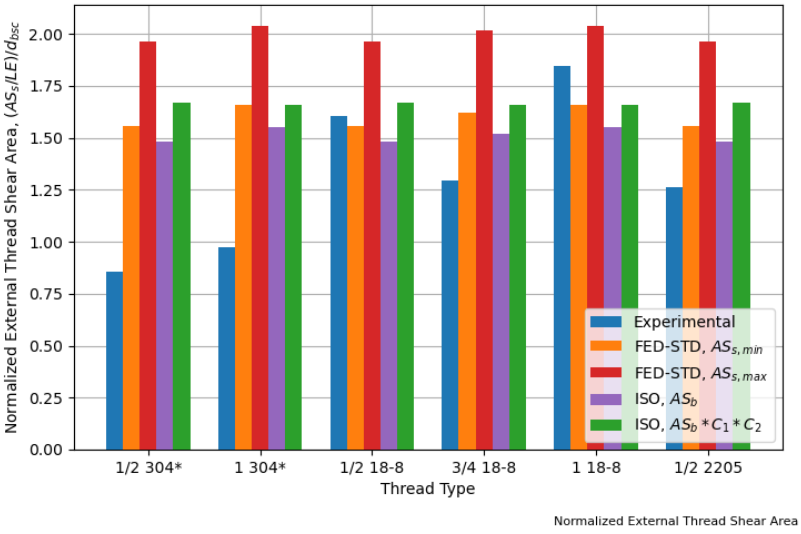


Figure 4.12. Normalized External Thread Shear Area (304*/18-8)

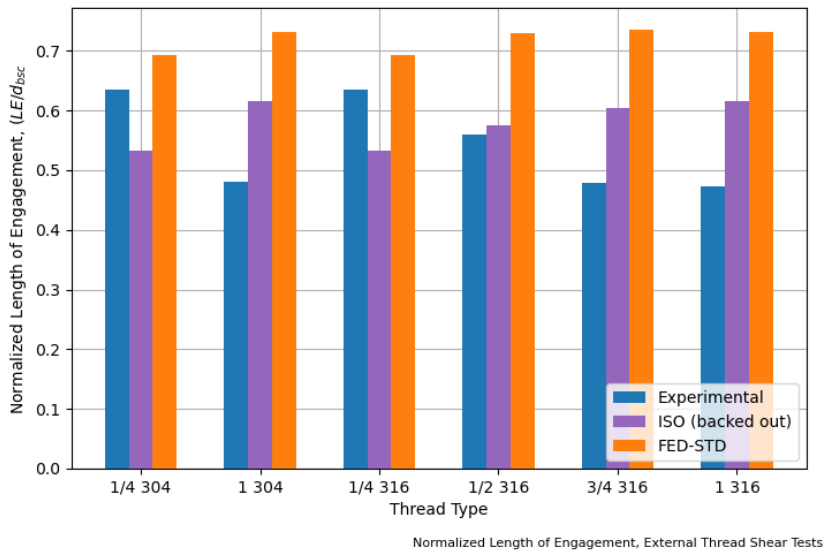


Figure 4.13. Normalized Length of Engagement (304/316)

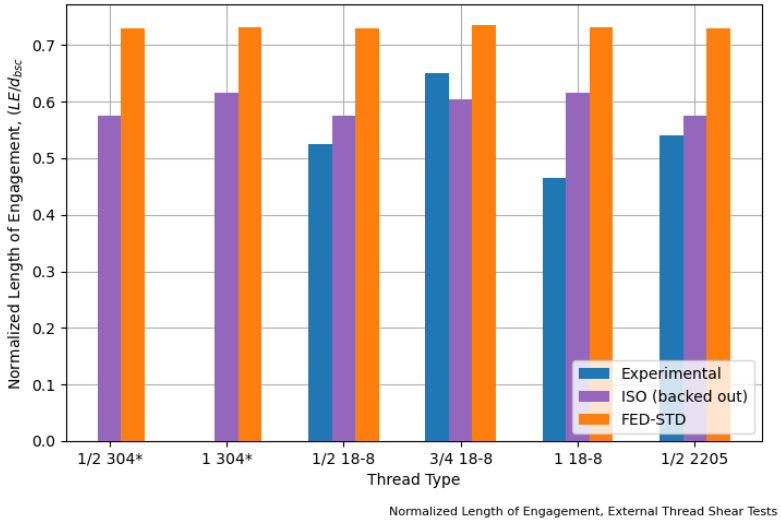


Figure 4.14. Normalized Length of Engagement (304*/18-8)

Table 4.5. Stainless Steel Shear Results

Lot	Shank (lbs)	Threads (lbs)	Ult. Stress (psi)	Shear/Tension Ratio
L015: 304 1/4-20	4475	2974	96509	0.962
L016: 304 1-8	67873	56722	87528	0.936
L032: 18-8 1/2-13	17112	13553	89397	0.890
L033: 18-8 3/4-10	38596	31451	89083	0.944
L034: 18-8 1-8	68233	56706	87900	0.954
			Mean	**0.9372**
			Std. Dev.	**0.0252**
L017: 316 1/4-20	4104	3086	87377	0.882
L018: 316 1/2-13	16833	13850	87795	0.846
L019: 316 3/4-10	35490	30902	81696	0.939
L020: 316 1-8	63711	57231	82290	0.916
			Mean	**0.896**
			Std. Dev.	**0.0352**
L021: ASTM A193 B8M 1-8	55843	47609	72674	0.87
L026: ASTM A193 B8M 1/2-13	13458	10576	70988	0.876
			Mean	**0.873**
			Std. Dev.	**0.003**
L035: 2205 Duplex 1/2-13	18802	12963	98154	0.829

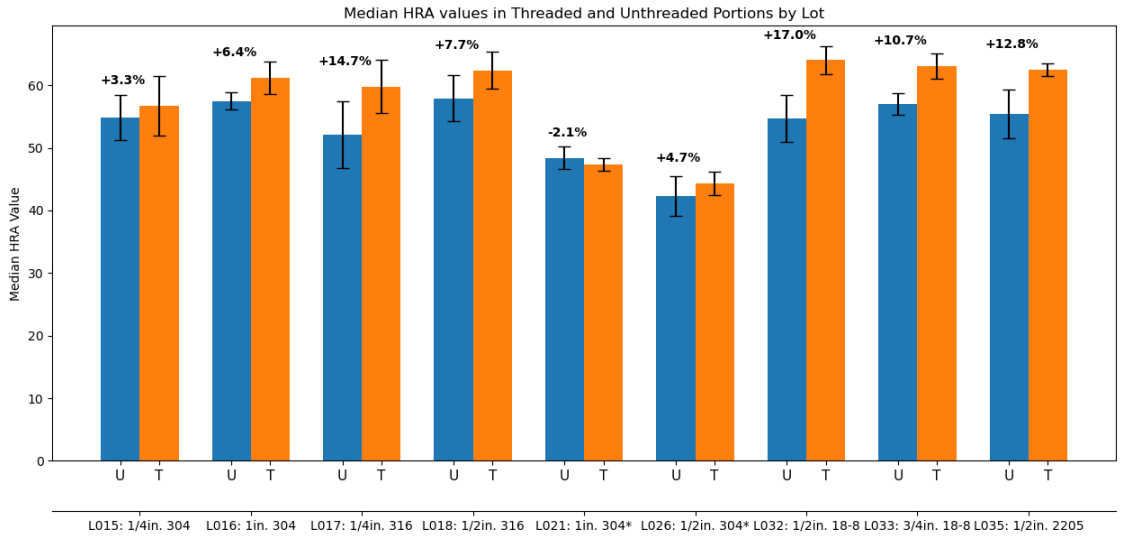


Figure 4.15. Median Hardness of Shank and Threads Compared

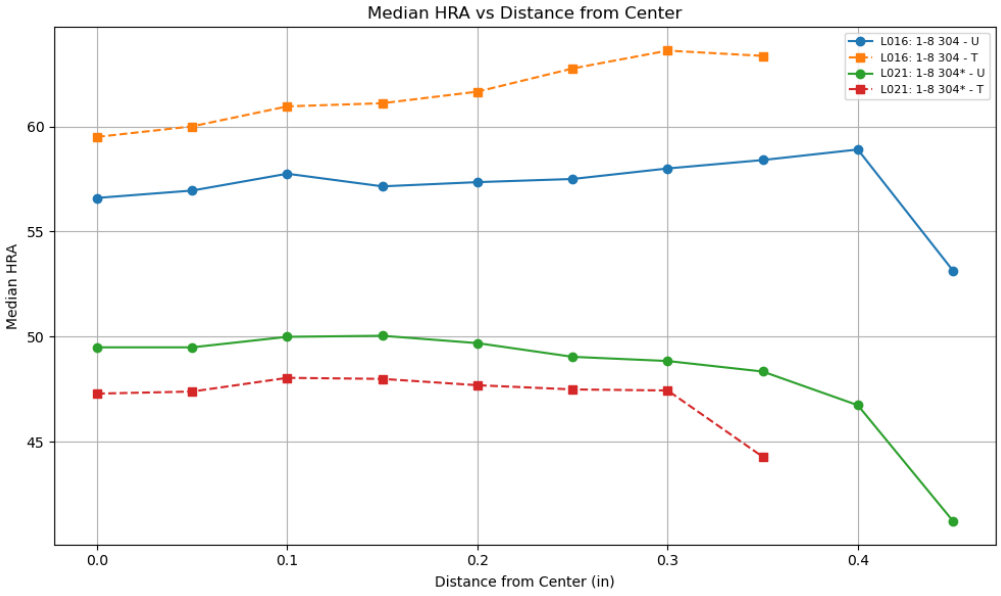


Figure 4.16. 1-8 Bolts Median HRA vs Distance from Center

CHAPTER FIVE

DISCUSSION

Tensile Strength

In the full specimen tensile testing, failure in the shank was observed for most lots. An example of this failure is pictured in **Figure 5.1.** Lots L021 and L026 did not experience tensile failure. Lot L035 (2205 Duplex) was the only lot to experience tensile failure in the threads. These observations align with those of previous studies (Song et al. 2020; Stranghöner and Abraham 2021).

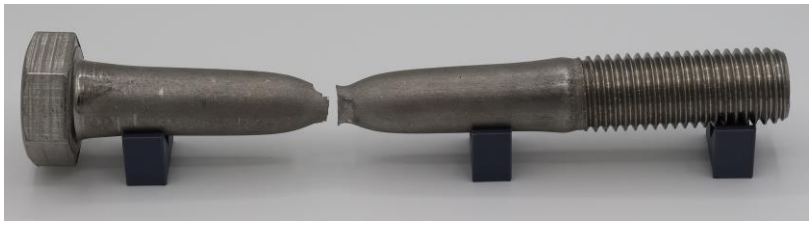


Figure 5.1. 304 Stainless 1-8 Type 0 Failure

Table 5.1 shows a comparison of experimental strength and a simplified tensile strength calculation. As expected, the experimental strength approximately equals the measured ultimate tensile stress and the basic area of the shank.

Table 5.1: Experimental Strength vs. Shank Area

Lot Number	P_{exp} (lbs)	F_u (psi)	A_{bsc} (in^2)	F_uA_{bsc}	P_{exp}/F_uA_{bsc}
L015	4689	100288	0.049	4923	0.953
L016	71578	93478	0.785	73417	0.975
L017	4656	99023	0.049	4861	0.958
L018	19836	103735	0.196	20368	0.974
L019	39285	87007	0.442	38439	1.022
L020	69316	89845	0.785	70564	0.982
L021	N/A	83505	0.785	65585	N/A
L026	N/A	81001	0.196	15904	N/A
L032	19026	100476	0.196	19728	0.964
L033	40248	94347	0.442	41681	0.966
L034	71367	92173	0.785	72393	0.986
L035	18213	118391	0.196	23246	0.783

Failure through the shank indicates that the strength of the material in the threaded region is greater than that in the shank by enough of a margin to force the failure into the larger cross-sectional area of the shank. Since failure did not occur through the threads, these tests can only provide a lower bound of the tensile strength in the threads. Assuming that the FED-STD tensile stress area (**Equation 2.1** or **Equation 2.2**) accurately represents the tensile stress area for stainless steel bolts, the ratio of ultimate strength in the threads to ultimate strength in the shank is greater than or equal to the ratio between the basic cross sectional area and the tensile stress areas. This ratio varies based on thread size. For example, for a 1-8 bolt the ratio is calculated as follows

$$A_{bsc} = \frac{\pi}{4}(1in)^2 = 0.7854in^2$$

$$A_s = \frac{\pi}{4}\left(1in - \frac{9\sqrt{3}}{16(8)}\right)^2 = 0.6057in^2$$

$$\frac{A_{bsc}}{A_s} = \frac{0.7854in^2}{0.6057in^2} = 1.297$$

For a 1/2-13 bolt, the ratio is calculated as follows

$$A_{bsc} = \frac{\pi}{4}(.5in)^2 = 0.1963in^2$$

$$A_s = \frac{\pi}{4}\left(.5in - \frac{9\sqrt{3}}{16(13)}\right)^2 = 0.1419in^2$$

$$\frac{A_{bsc}}{A_s} = \frac{0.7854in^2}{0.6057in^2} = 1.383$$

Therefore, for the 1 in. bolts, the material in the threads must be at least 29.7% stronger and 38.3% for the half inch. Using this same method, the ¼ in. and ¾ in. would require 54.4% and 32.3% respectively, and the mean is 38.7%. This estimated lower bound of the strength increase approximately equals the ratio between the test tensile stress area (TTSA, **Equation 4.1**) and the predicted TSA from the FED-STD (**Equation 2.1** and **Equation 2.2**). Grades 304/18-8 and 316 show a mean ratio of 1.375, with individual lots such as the 1/4-20 304 bolts reaching ratios as high as 1.55 (**Table 4.3**).

For bolts where failure occurs through the shank, use of the threaded tensile stress area is not appropriate and conservative. Based on information provided in the certificate of inspection it appears that the manufacturers were using the tensile stress area when reporting material strengths. One possibility for taking advantage of the increased strength is for the certificate of inspection to list failure mode and tensile strength.

External Thread Shear Strength and Length of Engagement

Taking a mean of the ratio between the tested ETSA and the FED-STD (A_{smin}) provides an ETSA ratio of 0.983 (**Table 4.4**). This value indicates that, at each length of engagement (LOE), materials with high RWH had, on average, 2.7% less ETSA than predicted by the FED-STD using A_{smin}. This difference in strength is essentially negligible, meaning the FED-STD (using $0.9F_u$) accurately predicts the strength at each LOE. It should be noted, however, that when using $0.6F_u$, this difference is an average of 47%, meaning the FED-STD underpredicts the strength by almost half when using the standard 0.6 shear ratio.

The effects of RWH on the required length of engagement (LOE) can be seen by comparing the experimental results to the FED standard using $0.6F_u$, shown in **Figure 4.13** and **Figure 4.14**. Required LOE is the length of engaged threads required to cause tensile failure of the bolt. An LOE under the required LOE may result in external thread shear. Given the previous results in ETSA, it would logically follow that RWH would decrease the required LOE as higher thread strength requires less thread engaged (lower ETSA) to reach the strength required to force the tensile failure to control. This is exactly what the results indicate. In the high RWH cases the required LOE is lower than the FED-STD calculation, as seen in **Figure 4.13** and **Figure 4.14**.

Strength of Low Work Hardened Stainless Steel Bolts

The two lots of 304 stainless steel that were ordered as bar stock (i.e., L021 and L026) appear to have been machined or forged rather than cold-rolled, suggesting that

although they have high WHP, they have low RWH compared to their “standard” 304 counterparts. Despite multiple attempts using varied setups, tensile failure could not be achieved for bolts from lots L021 and L026.

The initial test employed a 1-8 threaded washer, machined from pre-hardened 4140 steel, with a 1.0-inch length of engagement. The test followed the Full tension test method described in Chapter 3. As shown in **Figure 5.2**, the specimen failed via a thread-bending mode. The external threads deformed plastically, bent over, and ultimately pulled out of the fixture before reaching a load sufficient to induce tensile rupture. These threads are the threads following the 6 threads in the grip, as described in testing methods. Note that the test fixture was forcibly removed, causing damage to the remaining threads on the end of the bolt.

In the second test, to increase the likelihood of achieving tensile failure, a second threaded fixture was fabricated, this time with a 1.5-inch engagement length—a 50% increase over the first attempt. However, as seen in **Figure 5.3**, the same thread-bending failure occurred. The bolt threads yielded and bent under load, pulling out of the fixture without achieving tensile fracture. Once again, the 6 threads originally in the grip are noted, while three more pulled out during testing.

For a third test, the bolt was changed to a Lot L026 specimen (to verify repeatability between lots), and the fixture was changed to a standard steel nut rather than a fabricated washer, in an effort to conserve specialty parts. Again, as shown in **Figure 5.4**, the failure mode was identical—thread deformation and pull-out without tensile

failure. Following this third consistent result, further tensile testing on these lots was discontinued.

Though tensile failure was not achieved, the necking in the threaded portion is significant in all tests. This suggests that had the test been successful, the threaded portion would have controlled. This behavior further confirms the lack of RWH in these specimens and the more uniform material strength throughout both the threads and the shank.

The underlying cause of this failure mode appears to be related to the low ratio of yield stress to ultimate tensile stress in these two lots. As illustrated in **Figure 4.1**, this ratio is significantly lower in L021 and L026 than in the cold-formed, "standard" 304/18-8 lots. The bar-stock lots (L021 & L026) have a mean yield-to-ultimate ratio of 0.458, while the Cold-formed 304/18-8 lots have a mean yield-to-ultimate ratio of 0.593. This represents a 13.5% reduction in the yield-to-ultimate ratio, indicating a substantially lower yield strength relative to ultimate capacity. This reduced yield strength results in more ductile behavior during loading, particularly in the threaded portion engaged with the test fixture.

Two simultaneous conditions are hypothesized to drive the observed behavior: Progressive necking in the threaded region: The low yield strength promotes early plastic deformation beginning at the first engaged thread, initiating a necking sequence. As the load increases, the cross-sectional area of the threaded portion is reduced, diminishing engagement with the fixture and increasing susceptibility to bending.

Cascading Thread Bending and Pull-Out: As the leading thread yields and disengages, subsequent threads bear the load in sequence. These threads, rather than failing in shear, bend plastically and pull free, continuing the cascade. This explains why even a 50% increase in engagement length failed to force tensile rupture and resulted in the same failure as before.

Further increasing the engagement length was not feasible due to fixture limitations. The conclusion is that the low yield-to-ultimate ratio of these two lots leads to a successive, low-load thread-bending failure, preventing the application of sufficient force to induce tensile fracture.

To verify this, a simple comparison of the stress-strain relationship of each specimen is sufficient. A comparison of the stress strain relationships for standard stainless steel bolts: 304 1-8 (L016), 18-8 1/2-13 (L032), and 316 1-8 (L020) and stainless steel ordered from bar stock 304* 1-8 (L021) and 304* 1/2-13 (L026) is shown in **Figure 5.5.** The stress data for each specimen was normalized by the measured ultimate tensile strength of that specimen. The dashed lines present the yield stress, also normalized by the ultimate tensile strength. From this data, it can be seen that the ratio or yield to ultimate is lower for the 304 stainless steel bolts ordered from bar stock (13.5% lower on average). Numerical data is provided in **Table 4.2** for stainless steel bolts.

The shapes of the curves are also different. For lots L016, L020, and L032, the shift between the elastic and plastic regions of the curves is gradual. For lots L021 and L026, the shift is much more sudden and distinct. However, the behavior in the elastic

range is similar across the lots. Since the material composition of the bolts shown in **Figure 5.5** is the same (i.e., same work hardening potential), the differences in stress strain relationships can be attributed to the different manufacturing processes (i.e., different realized work hardening), specifically the lack of cold forming experienced by lots L021 and L026. The differences likely contributed to the abnormal behavior of the threaded region in the tension testing of lots L021 and L026.

Because tensile failure could not be achieved, the TSA ratio could not be used for classification. However, their ETSA ratios provide insight. While the "normal" 304/18-8 specimens had ETSA ratios ranging from 0.80 to 1.15, these two bar stock lots had a mean ratio of just 0.569. While the FED-STD (using A_{smin} and $0.9F_u$) accurately predicted ETSA at each length of engagement for high RWH bolts, for these two lots it overpredicted the ETSA significantly.

This case demonstrates the critical influence of manufacturing process on fastener performance. Even with identical alloy composition and nominal dimensions, a change in manufacturing can produce entirely different failure modes and mechanical behavior. It underscores the necessity of considering processing history when evaluating fastener performance, especially for materials with the potential for significant work hardening.

This conclusion is further supported by their noticeably lower ultimate tensile strengths. As shown in **Table 4.1**, the bar stock specimens had ultimate tensile values of 83 ksi and 80 ksi, while the other 304/18-8 specimens ranged from 92–100 ksi. The certified ultimate strength values provided by the manufacturer were much lower. This

rules out the possibility of error in the testing method or equipment and strengthens the conclusion that these lots, due to different manufacturing processes, have low RWH, even though their WHP is high.

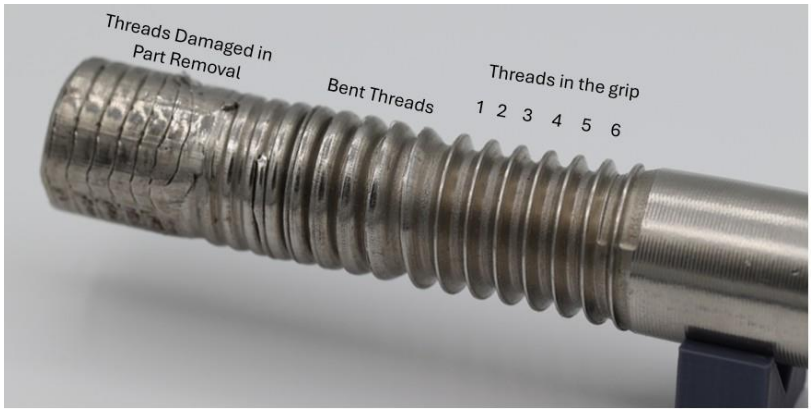


Figure 5.2. L021 1-8 Type 0 Test 1

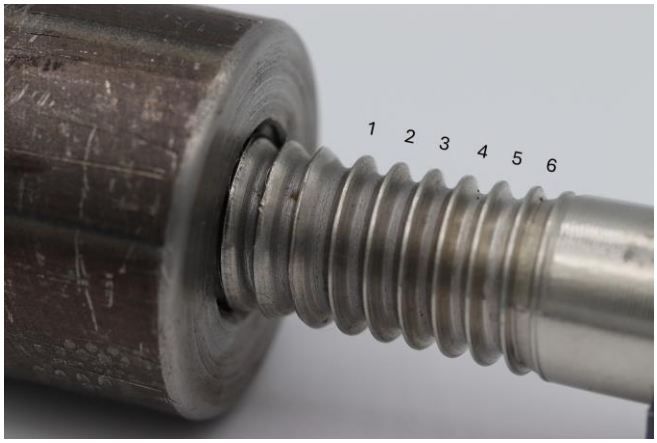


Figure 5.3. L021 1-8 Type 0 Test 2



Figure 5.4. L026 1/2-13 Type 0 Test 1

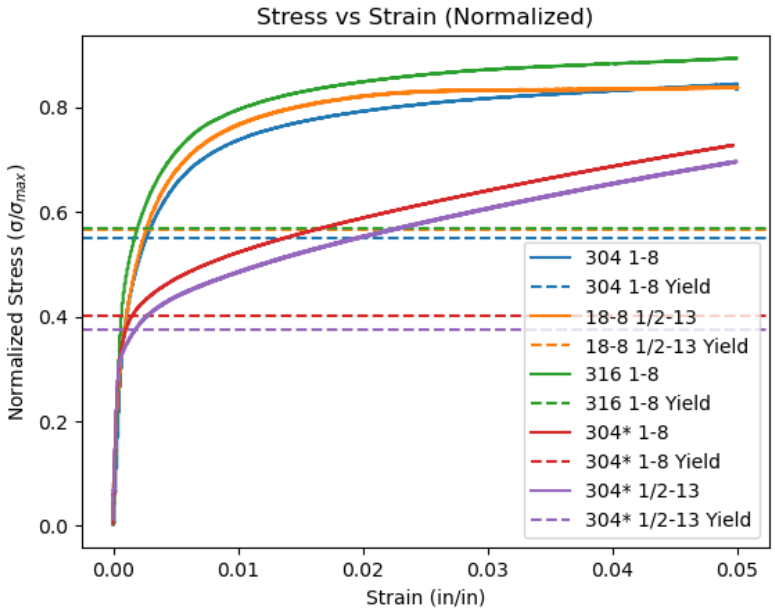


Figure 5.5. Stainless Steel Stress-Strain Curve Comparison

Cross Section Hardness Comparison

The hardness data provides direct evidence of difference in material properties at different cross sections and through the cross section. The primary discussion will center around the ½ inch and larger diameter bolts.

The hardness of both cross sections on the normal stainless-steel fasteners further this point. Across the 7 other lots, the median hardness of the threaded region was on average 10.37% higher than the shank (excluding the 1/4in. lots this average is 10.46%), as seen in **Figure 4.15**. While hardness is not a direct conversion to tensile strength, the correlation between higher hardness and higher tensile strength is unmistakable. A 10% increase in hardness in the same material (304) is linked to an increase in tensile strength of around 10%. The threaded region of the cold rolled specimens has a higher RWH and different material properties than the shank region, as opposed to the low RWH specimens where the shank and threaded region remain consistent to each other.

Furthermore, as seen in **Figure 4.16** the median hardness across the cross-section changes. Since work hardening in cold rolling is caused by deformations, the areas with higher level of deformation closer to the edges should receive increased material strength. This relationship is seen in the 1-8 304 cold rolled specimens. It should be noted that the final increment (test closest to the edge) generally results in a lowered value due to the lack or material confinement and easier indentation at the very edge of the bolt. The median hardness of the 304 specimen increases as the distance from center increases, as well as the shank being softer than the threads.

The median hardness for the 304* averaged a +1.3% difference between the shank and the threads, this difference is negligible and within the range of asserting that the material hardness in both sections is essentially constant. This verifies the previous findings that these specimens have low realized work hardening. The cross section of the

304* bolts in both the shank and the threads has not undergone significant cold-work hardening. The median hardness of the other 304* specimen shows the opposite. The median hardness of the shank is greater than that of the threads, but the median hardness also either remains the same or decreases across the cross section.

CHAPTER SIX

CONCLUSIONS AND RECOMMENDATIONS

This study investigated how work hardening influences the mechanical behavior of stainless steel fasteners, focusing on their tensile strength, external thread shear strength, and hardness. Existing design standards for fasteners are largely based on data from experiments on carbon steel bolts and do not fully capture the behavior of stainless steel bolts, which experience non-uniform strain-induced strengthening during manufacturing. By comparing measured performance to existing equations, this thesis sought to quantify the effects of work hardening on both material and geometric strength parameters. Several conclusions were drawn from the results presented:

- When tensile testing, there was failure through the shank in all lots execept L035 made from 2205 duplex stainless steel, resulting in strengths higher than predicted by standard equations
- Measured external thread shear strength was also higher than predicted by standard equations. A key reason for this was a higher than standard value of shear to tensile strength ratio, but work hardening effects also likley played a role.
- Length of engagement required to achieve tensile strength was lower than predicted by standard equations.

- Hardness measurements show direct evidence of differences in material properties due to work hardening between the shank and threads, as well as vartions within the cross section
- Minimally work hardened bolts did not exhibit tensile failure due to extreme plastic thread behavior.

These findings clarify how stainless steel fasteners should be understood and designed. They demonstrate that the enhanced strength and altered failure behavior of stainless bolts arise from cold-working effects rather than inherent alloy properties alone. Consequently, equations and assumptions derived from carbon steel data are not fully applicable to stainless steels. Incorporating work-hardening effects into design equations and standards would allow engineers to predict connection behavior more accurately, ensuring both safety and material efficiency. This research provides an empirical foundation for such revisions and establishes a framework for future evaluation of fasteners with varying degrees of work hardening and manufacturing histories.

REFERENCES

ASTM. 2021. Standard Test Methods for Determining the Mechanical Properties of Externally and Internally Threaded Fasteners, Washers, Direct Tension Indicators, and Rivets. ASTM F606-21. West Conshohocken, Pennsylvania: ASTM International.`

ASTM. 2022. Standard Test Methods for Tension Testing of Metallic Materials. ASTM E8/E8M-22. West Conshohocken, Pennsylvania: ASTM International.

ASTM. 2025. Standard Test Methods for Rockwell Hardness of Metallic Materials. ASTM E18-25. West Conshohocken, Pennsylvania: ASTM International.

Atkinson, M. 1984. "Strain hardening behavior of polycrystalline iron and low-carbon steels—A statistical analysis." Metall Trans A, 15 (6): 1185–1192. https://doi.org/10.1007/BF02644713.

Cook, D. C. 1987. "Strain induced martensite formation in stainless steel." Metall Trans A, 18 (2): 201–210. https://doi.org/10.1007/BF02825701.

Dolinšek, S. 2003. "Work-hardening in the drilling of austenitic stainless steels." Journal of Materials Processing Technology, 7th International Scientific Conference: Achievements in Mechanical & Materials Engineering, 133 (1): 63–70. https://doi.org/10.1016/S0924-0136(02)00245-5.

Fan, Z., H. Mingzhi, and S. Deke. 1989. "The relationship between the strain-hardening exponent n and the microstructure of metals." Materials Science and Engineering: A, 122 (2): 211–213. https://doi.org/10.1016/0921-5093(89)90632-1.

GSA. 1991. Federal Standard: Screw-Thread Standards for Federal Services Section 2 Unified Inch Screw Threads - UN and UNR Thread Forms. FED-STD-H28/2B. Washington, DC: Federal Supply Services, General Services Administration.

ISO. 2012. ISO/TR 16224: Technical Aspects of Nut Design. ISO/TR 16224. Geneva, Switzerland: International Organization for Standardization.

Koehler, J. S. 1952. "The Nature of Work-Hardening." Phys. Rev., 86 (1): 52–59. https://doi.org/10.1103/PhysRev.86.52.

Llewellyn, D. T. 1997. "Work hardening effects in austenitic stainless steels." Materials Science and Technology, 13 (5): 389–400. SAGE Publications. https://doi.org/10.1179/mst.1997.13.5.389.

Lo, K. H., C. H. Shek, and J. K. L. Lai. 2009. "Recent developments in stainless steels." Materials Science and Engineering: R: Reports, 65 (4–6): 39–104. https://doi.org/10.1016/j.mser.2009.03.001.

MatWeb. 2025. "MatWeb." MatWeb Material Property Data. https://www.matweb.com/.

Song, Y., J. Wang, B. Uy, and D. Li. 2020. "Stainless steel bolts subjected to combined tension and shear: Behaviour and design." Journal of Constructional Steel Research, 170: 106122. https://doi.org/10.1016/j.jcsr.2020.106122.

Stranghöner, N., and C. Abraham. 2021. "Shear resistance of austenitic and duplex stainless steel bolts." Journal of Constructional Steel Research, 184: 106807. https://doi.org/10.1016/j.jcsr.2021.106807.

Wood, W. A. 1940a. “Crystalline structure and deformation of metals.” Proc. Phys. Soc., 52 (1): 110. https://doi.org/10.1088/0959-5309/52/1/316.

Wood, W. A. 1940b. “Crystalline structure and deformation of metals.” Proc. Phys. Soc., 52 (1): 110–116. https://doi.org/10.1088/0959-5309/52/1/316.

Zhang, Z., W. Zhao, Q. Sun, and C. Li. 2006. “Theoretical calculation of the strain-hardening exponent and the strength coefficient of metallic materials.” J. of Materi Eng and Perform, 15 (1): 19–22. https://doi.org/10.1361/10599490524057.

VITA

Pierce R. Okken is an Air Force Civil Engineering Officer, who received his undergraduate degree in Civil Engineering from the United States Air Force Academy in Colorado Springs, CO. He also worked for 4 years in residential general contracting prior to achieving a commission in the US Air Force. His professional interests are structural engineering and steel construction. Outside of professional life, he enjoys running with his wife, playing guitar, long-range precision rifle shooting, and reading the founding documents of America to his daughter.